Research Article

Fast implementation of sparse iterative covariance-based estimation for processing MST radar data

C. Raju[1] · T. Sreenivasulu Reddy[1] · G. Ramachandra Reddy[2]

Abstract

Doppler estimation is an essential problem for the mesosphere–stratosphere–troposphere (MST) radar data for estimation of atmospheric parameters. The Doppler is estimated by computing the power spectral density using either parametric or non-parametric method. A recent class of spectral estimation technique referred as Sparse Iterative Covariance Based Estimation (SPICE) is introduced in literature. SPICE is a sound, user-parameter free, good resolution, iterative and globally convergent method which exhibits the enhanced results than the current spectral estimation methods, at the high computational cost. This letter presents the fast implementation of the SPICE algorithm for the MST radar data and the estimation of various wind parameters at a lesser computational time and is validated with the radiosonde data.

Keywords MST radar · SPICE · Gohberg–Semencul (GS) factorization · Spectrum estimation

1 Introduction

Spectrum estimation has wide range of applications [1]. Different spectral estimation methods have been developed to solve the problems, and they may be classified as nonparametric, parametric and semiparametric.

The nonparametric methods for spectrum estimation do not presume any model (deterministic or statistical) for data, except that it is zeroed outside the observation interval. A very well-known nonparametric method is the periodogram which is defined as

$$\hat{\Phi}(k) = \frac{1}{N}\left|\sum_{n=0}^{N-1} x(n)e^{-j\frac{2\pi k}{N}n}\right|^2, \quad k = 0, 1, \ldots, N-1 \tag{1}$$

where N is the number of sample points, $\{x(n)\}_{n=0}^{N-1}$ are the observed samples of a signal. The nonparametric methods endure fundamental limitations. In the recent times, SPICE (Semiparametric/Sparse Iterative Covariance-based Estimation), a novel method for spectral estimation has been proposed [2], which is developed from the ideas of sparse estimation. This method is a user parameter free iterative technique that gives superior resolution. It is globally convergent and has minor sidelobe levels. However, it suffers from high computational complexity. SPICE is an iterative algorithm. In this paper, we present a method to reduce the computational load of SPICE algorithm which is based on Gohberg–Semencul (GS) Factorization. The inverse of the sample covariance matrix $\mathbf{R}$ is decomposed by GS factorization and the fast schemes are used for computation of $\mathbf{R}^{-1}\boldsymbol{x}$. The Toeplitz structure of $\mathbf{R}$ is exploited for efficient manipulation of the matrix in each iteration. After GS factorization, a Fast Fourier Transform (FFT) is applied to still improve the computational speed of spectral estimation algorithm.

The MST radar data retrieved from the "National Atmospheric Research laboratory" (NARL) is an evenly spaced complex signal containing both in-phase (I) and quadrature (Q) phase components. The wind data provided by NARL in atmospheric regions of the mesosphere, stratosphere and

✉ C. Raju, c.raju1131@gmail.com | [1]Department of ECE, Sri Venkateswara University College of Engineering, S.V. University, Tirupati, Andhra Pradesh 517 502, India. [2]School of Electronics Engineering, Vellore Institute of Technology University, Vellore, Tamil Nadu 632 014, India.

SN Applied Sciences (2019) 1:998 | https://doi.org/10.1007/s42452-019-0930-5

Received: 22 February 2019 / Accepted: 16 July 2019

Published online: 08 August 2019

troposphere, starting from 3.6 km, maintains a resolution of 150 m. The "Atmospheric Data Processor" (ADP) is found to give an agreeable Doppler profile up to a height of 11 km where noise is less. Since the lower stratosphere extends from 10 to 20 km above the earth's surface, any spectrum estimating algorithm is expected to give good results in this particular range. There arises a need to go for a better functioning spectrum estimation method, especially at the height range of 14–17 km, as the existing methods [3–6] at this height fail to estimate the power spectrum accurately. Hence, semiparametric techniques can be focused on to improve the spectral estimation accuracy even for ill-conditioned data.

In this letter, vectors are represented using the lowercase bold letters and the matrices using the uppercase boldface. The scalars are indicated using the normal letters. Notations $|\cdot|, \|\cdot\|, (\cdot)^*, (\cdot)^T$, and $E(\cdot)$ represents the modulus, Frobenius norm, Hermitian transpose (complex conjugate transpose), the transpose and the expectation respectively. The subscript $[.]_k$ denotes the vector kth element, and $\boldsymbol{I}_N$ represents an identity matrix of order N.

2 Review of spice algorithm

SPICE is a newly introduced technique for the sparse signal recovery based on the covariance fitting criterion. It is a hyper parameter free and gives better performance than other methods.

Let y_n be the complex signal data, which is the weighted combination of C complex exponentials with frequencies

$$\{\Omega_r\}_{r=1}^{N} \epsilon [0, \Omega_{max}]$$

$$y_n = \sum_{r=1}^{C} q_r e^{j\omega_r t_n} + \varepsilon_n \tag{2}$$

where C is a constant, $\{t_n\}_{n=1}^{N}$ representing the instants of sampling time that can be irregularly spaced. The magnitude of the rth frequency component Ω_r is q_r, $\varepsilon(t_n)$ is the "additive white gaussian noise" component related to the n^{th} sampling time. Let $R \gg C$, be the number of frequency points that the frequency axis is sampled.

Then the complex signal can be replicated as

$$\boldsymbol{y} = \sum_{r=1}^{R} \boldsymbol{d}(\omega_r) q_r + \boldsymbol{\varepsilon} \tag{3}$$

$$\text{where } \boldsymbol{y} = [y_1, y_2, \dots, y_N]^T \tag{4}$$

$$\begin{aligned} \boldsymbol{D} &= [\boldsymbol{d}(\omega_1), \boldsymbol{d}(\omega_2), \dots, \boldsymbol{d}(\omega_N)]^T \text{ with} \\ \boldsymbol{d}(\omega_r) &= [e^{j\omega_1 t_1}, \dots ., e^{j\omega_r t_N}] = \boldsymbol{d_r} \end{aligned} \tag{5}$$

$\boldsymbol{q} = [q_1, q_2, \dots, q_R]^T$, $|q_r|^2$ is the power value corresponding to the rth frequency component that is to be calculated.

$$\varepsilon = [\varepsilon_1, \varepsilon_2, \dots, \varepsilon_N]^T \tag{6}$$

where $\varepsilon_1 = \varepsilon_2 = \dots = \varepsilon_N = \sigma^2$, σ^2 is the noise variance.

The $N \times N$ covariance matrix $\boldsymbol{R}_N$ of the received signal is given as

$$\boldsymbol{R}_N = E(\boldsymbol{yy}^*) = \sum_{r=1}^{R} |q_r|^2 \boldsymbol{d}_r \boldsymbol{d}_r^* + E(\boldsymbol{\varepsilon\varepsilon}^*) = \boldsymbol{DPD}^* \tag{7}$$

$$\text{where } \boldsymbol{D} = [\boldsymbol{d}_1 \boldsymbol{d}_2 \boldsymbol{d}_3 \dots ..\boldsymbol{d}_R \boldsymbol{I}_N] = [\boldsymbol{d}_1 \dots \dots ..\boldsymbol{d}_{R+N}]$$

$$\boldsymbol{P} = diag(m_1, m_2, \dots ., m_{R+N}) \tag{8}$$

$$\text{where } m_r = \begin{cases} |q_r|^2, & r = 1, 2, \dots R \\ \sigma^2, & r = R+1, R+2, \dots, R+N \end{cases}; \tag{9}$$

$$E(\boldsymbol{\varepsilon\varepsilon}^*) = \sigma^2 \boldsymbol{I}_N \tag{10}$$

The SPICE algorithm is based on minimizing the weighted covariance function f.

$$f = \left\| \boldsymbol{R}_N^{-1/2} (\hat{\boldsymbol{R}}_N - \boldsymbol{R}_N) \right\|^2 \tag{11}$$

where $\boldsymbol{R}_N^{-1/2}$ represents the Hermitian square root of $\boldsymbol{R}_N^{-1}$, $\|\cdot\|$ denotes the Frobenius norm.

SPICE estimate [7, 8] of the m_r's is an iterative process of the form:

$$m_r(i+1) == \frac{m_r(i) \left| \boldsymbol{d}_r^* \boldsymbol{R}_N^{-1}(\boldsymbol{i}) \boldsymbol{y} \right|}{w_r^{\frac{1}{2}} \rho(i)} \tag{12}$$

$$w_r = \frac{\|\boldsymbol{d}_r\|^2}{\|\boldsymbol{y}\|^2} \tag{13}$$

$$\rho(i) = \sum_{s=1}^{R+N} w_s^{\frac{1}{2}} m_s(i) \left| \boldsymbol{d}_s^* \boldsymbol{R}_N^{-1}(\boldsymbol{i}) \boldsymbol{y} \right| \tag{14}$$

where i is the iteration number and $m_r(i)$ is the estimate of m_r at the ith iteration. The method is initialized with an initial estimate of the m_r's, i.e., $m_r(0) = \frac{|\boldsymbol{d}_r^* \boldsymbol{y}|^2}{\|\boldsymbol{d}_r\|^4}$ similar to the periodogram.

The computational complexity of $\mathcal{O}(N^2R)$ increases with increase in signal points N and frequency domain sampling points R. In the next section we introduce a method to reduce the computational complexity of the algorithm.

3 Implementation of spice algorithm using Gohberg–Semencul Factorization (SPICE_GS)

The computational complexity of the algorithm, to a much extent, depends on the computation of $\boldsymbol{u} = \boldsymbol{R}_N^{-1}\boldsymbol{y}$. The direct implementation of SPICE does not take into account the Toeplitz arrangement of Hermitian matrix $\boldsymbol{R}_N$. Based on GS factorization [9–13] the inverse of covariance matrix $\mathbf{R}_\mathrm{N}$ is denoted by a sequence of the Toeplitz matrices. The matrix product can be enhanced by this factorization. The Levinson–Durbin algorithm (LDA) and the Fast Fourier Transform can be employed to increase the computational speed.

3.1 Fast computation of the covariance matrix $\boldsymbol{R}_N$

The covariance matrix of observed data is defined as $\boldsymbol{R}_N = E(\boldsymbol{y}\boldsymbol{y}^*) = \boldsymbol{DPD}^*$.

We rewrite $\boldsymbol{R}_N$ as

$$\mathbf{R}_\mathrm{N} = \begin{bmatrix} r_0 & r_1 & \cdots & r_{N-1} \\ r_{-1} & r_0 & \cdots & \vdots \\ \vdots & \vdots & \ddots & r_1 \\ r_{-N+1} & \cdots & r_{-1} & r_0 \end{bmatrix} = \begin{bmatrix} r_0 & r_1 & \cdots & r_{N-1} \\ r_1^* & r_0 & \cdots & r_{N-2} \\ \vdots & \vdots & \ddots & \vdots \\ r_{N-1}^* & r_{N-2}^* & \cdots & r_0 \end{bmatrix} = \sum_{r=1}^{R+N} m_r d_r d_r^H \tag{15}$$

where $r_{-m} = r_m^*$, m = 0,1,… N − 1.

Each element of the Eq. (15) is specified by $r_n = \sum_{r=0}^{K-1} m_r e^{-j2\pi nr/K}$, $n = 0, 1, 2, \dots, N-1$ which indicates that $\{r_m\}_{m=0}^{N-1}$ are the first elements of the K-point FFT of $\{m_r\}_{r=0}^{K-1}$, where $K = (R + N)$.

Using the first N values of the FFT of m_r, $\boldsymbol{R}_N$ can be formulated. This requires $\mathcal{O}(K \log_2(K))$ flops.

3.2 Fast computation of $\mathbf{R}_\mathrm{N}^{-1}\mathbf{y}$

As soon as the first column of $\boldsymbol{R}_N$ is presented, the vector $\boldsymbol{u}$ can be involved in the linear equation $\boldsymbol{R}_N\boldsymbol{u} = \boldsymbol{y}$.

The fast computation of $\boldsymbol{R}_N^{-1}$ will help to reduce the computational complexity of SPICE algorithm. There are two approaches to compute $\boldsymbol{R}_N^{-1}$ taking into account the Hermitian Toeplitz structure of $\boldsymbol{R}_N$. The first approach is based on Choleskey decomposition, where the inverse of the correlation matrix of order N is given in terms of all the autoregressive (AR) coefficients up to order $N-1$. The second approach uses Gohberg–Semencul (GS) factorization [14, 15] to compute the inverse using only AR coefficients of order $N-1$ which is described below.

3.2.1 The Gohberg–Semencul Relation

Let us proceed in the following way to express $\boldsymbol{R}_N^{-1}$ only in terms of the coefficients of prediction error filter of order $N-1$ $(i.e., 1, a_{N-1}(1), \dots, a_{N-1}(N-1))$.

First, we built a positive definite Hermitian Toeplitz matrix of size $2N \times 2N$.

$$\boldsymbol{G} = \left[\begin{array}{cccc|cccc} r_0 & r_1 & \cdots & r_{N-1} & r_N & r_{N+1} & \cdots & r_{2N-1} \\ r_1^* & \ddots & \cdots & r_{N-2} & r_{N-1} & \ddots & \cdots & \vdots \\ \vdots & \vdots & \ddots & \vdots & \vdots & \vdots & \ddots & \vdots \\ r_{N-1}^* & \cdots & \cdots & r_0 & r_1 & \cdots & \cdots & r_N \\ \hline r_N^* & r_{N-1}^* & \cdots & r_1^* & r_0 & r_1 & \cdots & r_{N-1} \\ \vdots & \vdots & \cdots & \vdots & \vdots & \vdots & \ddots & \vdots \\ r_{2N-1}^* & \cdots & \cdots & r_N^* & r_{N-1}^* & \cdots & r_1 & r_0 \end{array}\right] \tag{16}$$

where the values $r_N, r_{N+1}, \dots, r_{2N-1}$ are recursively computed using Yule-Walker equation

$$r_k = -\sum_{i=1}^{N-1} a_{N-1}(i) r_{k-1} \quad for\ k = N, N+1, \dots, 2N-1.$$

Let us define $\boldsymbol{L}_1$ and $\boldsymbol{L}_2$ as $N \times N$ lower triangular Toeplitz matrices

$$\boldsymbol{L}_1 = \begin{bmatrix} 1 & 0 & \cdots & 0 \\ a_{N-1}^*(1) & 1 & \cdots & \vdots \\ a_{N-1}^*(2) & a_{N-1}^*(1) & \cdots & \vdots \\ \vdots & \ddots & \ddots & \vdots \\ a_{N-1}^*(N-1) & \cdots & \cdots & 1 \end{bmatrix}, \quad \boldsymbol{L}_2 = \begin{bmatrix} 0 & 0 & \cdots & 0 \\ a_{N-1}(N-1) & 0 & \cdots & \vdots \\ a_{N-1}(N-2) & a_{N-1}(N-1) & \cdots & \vdots \\ \vdots & \ddots & \ddots & \vdots \\ a_{N-1}(1) & a_{N-1}(2) & \cdots & 0 \end{bmatrix} \tag{17}$$

Let $\boldsymbol{X}$ be $2N \times 2N$ matrix, $\boldsymbol{X} = \left[\begin{array}{c|c} \boldsymbol{L}_1 & O \\ \hline \boldsymbol{L}_2^H & \boldsymbol{A}_N \end{array}\right]$

Observe that $(N+1)$ left columns of $\boldsymbol{X}$ have Toeplitz structure, and $\boldsymbol{GX} = \boldsymbol{YZ}$ where $\boldsymbol{Y}$ is a $(2N \times 2N)$ upper triangular matrix with unity elements in its main diagonal and $\boldsymbol{Z}$ is $(2N \times 2N)$ diagonal matrix.

$$\boldsymbol{Z} = diag[\epsilon(N-1), \epsilon(N-1), \ldots., \epsilon(N-1), \epsilon(N-2), \epsilon(N-2), \ldots., \epsilon(1), \epsilon(0)]$$

Since $\boldsymbol{X}^H$ and $\boldsymbol{GX}$ are upper triangular and since $\boldsymbol{X}^H\boldsymbol{GX}$ is Hermitian, it results in $\boldsymbol{X}^H\boldsymbol{GX} = \boldsymbol{Z}$ and $\boldsymbol{G}^{-1} = \boldsymbol{XZ}^{-1}\boldsymbol{X}^H$.

Thus

$$\boldsymbol{G}^{-1} = \left[\begin{array}{c|c} \boldsymbol{L}_1 & O \\ \hline \boldsymbol{L}_2^H & \boldsymbol{A}_N \end{array}\right] \begin{bmatrix} \epsilon^{-1}(N-1) & 0 & \cdots & 0 \\ 0 & \epsilon^{-1}(N-1) & \cdots & \vdots \\ \vdots & \vdots & \ddots & \vdots \\ 0 & \cdots & \cdots & \epsilon^{-1}(0) \end{bmatrix} \left[\begin{array}{c|c} \boldsymbol{L}_1^H & \boldsymbol{L}_2 \\ \hline O & \boldsymbol{A}_N^H \end{array}\right]$$

$$\boldsymbol{G}^{-1} = \left[\begin{array}{c|c} \epsilon^{-1}(N-1)\boldsymbol{L}_1\boldsymbol{L}_1^H & \epsilon^{-1}(N-1)\boldsymbol{L}_1\boldsymbol{L}_2 \\ \hline \epsilon^{-1}(N-1)\boldsymbol{L}_2^H\boldsymbol{L}_1^H & \epsilon^{-1}(N-1)\boldsymbol{L}_2^H\boldsymbol{L}_2 + \boldsymbol{R}_N^{-1} \end{array}\right] \tag{18}$$

Since $\boldsymbol{R}_N$ and $\boldsymbol{G}$ are Hermitian Toeplitz matrices, they are centro-Hermitian and their inverses are also centro-Hermitian.

Applying this to (18), we obtain

$$\epsilon^{-1}(N-1)\boldsymbol{J}\boldsymbol{L}_1\boldsymbol{L}_1^H\boldsymbol{J} = \epsilon^{-1}(N-1)\left(\boldsymbol{L}_2^H\boldsymbol{L}_2\right)^* + \left(\boldsymbol{R}_N^{-1}\right)^* \tag{19}$$

where $\boldsymbol{J}$ is a $(N \times N)$ exchange matrix with unity elements in the cross diagonal and zeros elsewhere. Since $\boldsymbol{J}^2 = \boldsymbol{I}$ and $\boldsymbol{JR}_N^{-1}\boldsymbol{J} = \left(\boldsymbol{R}_N^{-1}\right)^*$

$$\epsilon^{-1}(N-1)\boldsymbol{L}_1\boldsymbol{L}_1^H = \epsilon^{-1}(N-1)\left(\boldsymbol{J}\left(\boldsymbol{L}_2^H\right)^*\boldsymbol{J}\right)\left(\boldsymbol{J}\boldsymbol{L}_2^*\boldsymbol{J}\right) + \boldsymbol{R}_N^{-1} \tag{20}$$

Using the fact that $\boldsymbol{J}\left(\boldsymbol{L}_2^H\right)^*\boldsymbol{J} = \boldsymbol{L}_2 \& \boldsymbol{J}\boldsymbol{L}_2^*\boldsymbol{J} = \boldsymbol{L}_2^H$,

$$\text{We get } \boldsymbol{R}_N^{-1} = \frac{1}{\epsilon(N-1)}\left[\boldsymbol{L}_1\boldsymbol{L}_1^H - \boldsymbol{L}_2\boldsymbol{L}_2^H\right] \tag{21}$$

which is the G–S relation.

The matrices $\boldsymbol{L}_1$ and $\boldsymbol{L}_2$ involved in $\boldsymbol{R}_N^{-1}$ are Toeplitz matrices, hence $\boldsymbol{R}_N^{-1}\boldsymbol{y}$ can be computed using FFT, as a Toeplitz matrix operating on a vector can be viewed as linear convolution operation and linear convolution can be converted into equivalent circular convolution by appropriate modifications to $\boldsymbol{L}_1$ and $\boldsymbol{L}_2$ matrices and the vector $\boldsymbol{y}$. Thus, $\boldsymbol{R}_N^{-1}\boldsymbol{y}$ can be computed with an order of $N\log_2 N$ flops. The L–D algorithm needs N^2 flops. Thus the order of flops needed to compute $\boldsymbol{R}_N^{-1}\boldsymbol{y}$ will be $N\log_2 N + N^2$.

Table 1 Levinson–Durbin algorithm for computing AR coefficients and prediction error

Step no.	Operation
1.	Initialize the recursion $a(0) = 1, \epsilon(0) = r_0$
2.	For $i = 0, 1, \ldots, N-2$ $r_i = r_{i+1} + \sum_{j=1}^{i} a_i(j) r_{i-j+1}, \Gamma_{i+1} = -\frac{r_i}{\epsilon(i)}$ For $j = 1, 2, \ldots, i$ $a_{i+1}(j) = a_i(j) + \Gamma_{i+1}a_i^*(i-j+1)$ $a_{i+1}(i+1) = \Gamma_{i+1}$ $\epsilon(i+1) = \epsilon(i)\left[1 - \left\|\Gamma_{i+1}\right\|^2\right]$

The efficient implementation of the SPICE algorithm for MST radar is outlined as follows:

For each iteration of SPICE_GS,

1. Compute the initial power estimate $\{m_r\}$ through $(R+N)$ point FFT of the data vector $\boldsymbol{y}$.
   i.e., $m_r(i) = |FFT(\boldsymbol{y})|^2, r = 0, 1, 2, \ldots, K-1$.
2. To formulate $\boldsymbol{R}_N$, first compute $r_n(i) = \sum_{r=0}^{K-} m_r(i)e^{j\frac{2\pi nr}{K}}, n = 0, 1, \ldots, N-1$ which indicates that $\{r_n\}_{n=0}^{N-1}$ are first elements of K-point IFFT of $\{m_r\}_{r=0}^{K-1}$ where $K = R + N$.
   Using $r_n(i)$ values, $\boldsymbol{R}_N$ can be formulated as it is Hermitian Toeplitz matrix.
3. Given $r_n, n = 0, 1, \ldots, N-1, \epsilon(N-1)$, compute AR coefficients of order $(N-1)$ using L–D
   Algorithm given in Table 1. Using AR coefficients $\boldsymbol{L}_1$ and $\boldsymbol{L}_2$ matrices can be formulated and
   $\boldsymbol{u} = \boldsymbol{R}_N^{-1}\boldsymbol{y}$ can be computed as $\boldsymbol{u} = \frac{1}{\epsilon(N-1)}\left[\boldsymbol{L}_1\boldsymbol{L}_1^H - \boldsymbol{L}_2\boldsymbol{L}_2^H\right]\boldsymbol{y}$.
4. Calculate $w_r^{\frac{1}{2}} = \frac{\|\boldsymbol{d}_r\|}{\|\boldsymbol{y}\|}$ and $c_r = \left|\boldsymbol{d}_r^*\mathbf{u}\right|, \rho = \sum_{l=1}^{R+N} w_l^{\frac{1}{2}} m_l c_l$.
5. Update the power values $m_r \leftarrow m_r c_r / w_r^{\frac{1}{2}} \rho$ till the convergence criterion is met.

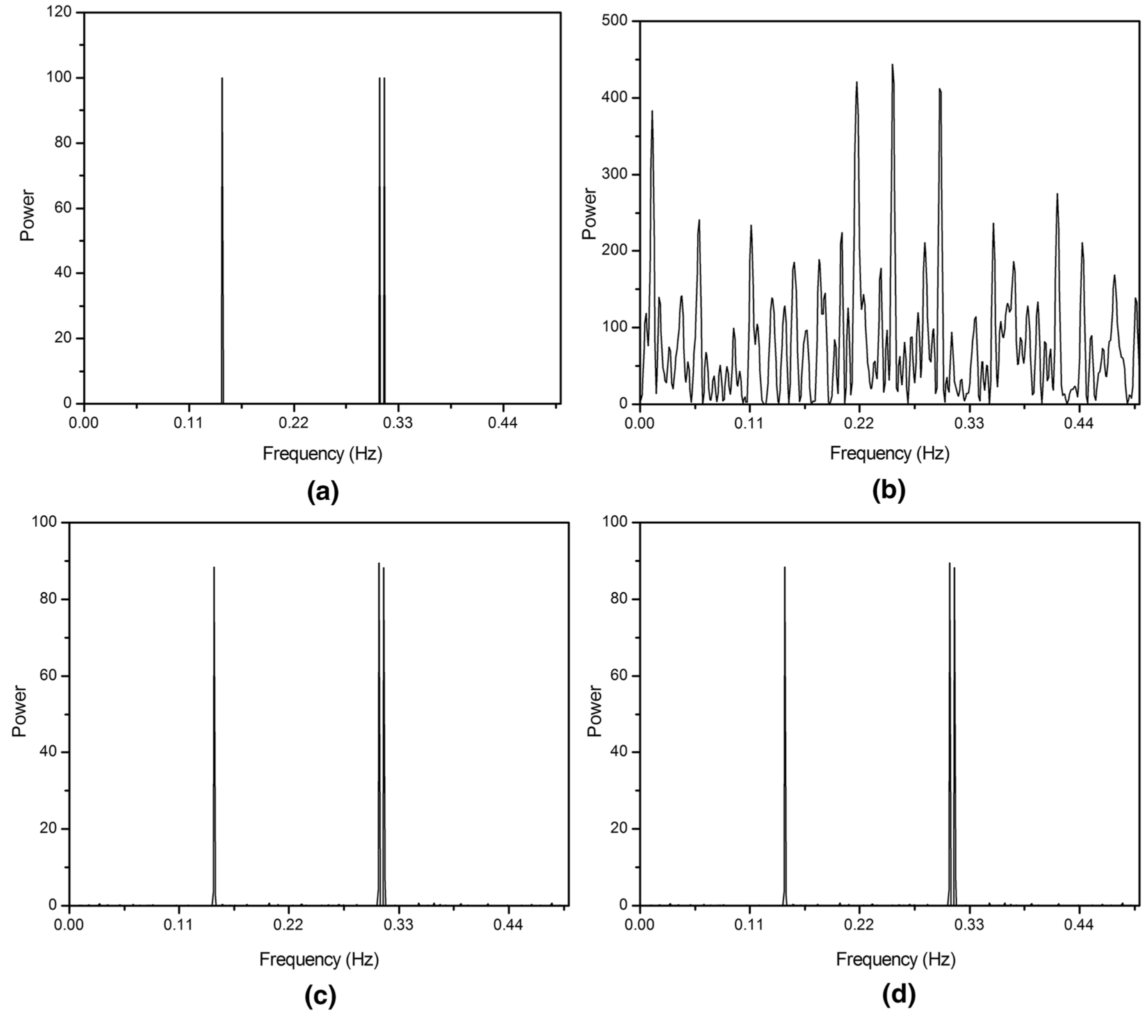

Fig. 1 **a** Spectrum of the original signal; **b** power Spectrum using periodogram; **c** SPICE; **d** SPICE_GS

Table 2 The main operation process of SPICE and SPICE_GS

Method	Step	Computational complexity
SPICE	Covariance matrix calculation	N^2R
	Inverse covariance matrix	N^2R
SPICE_GS	Covariance matrix calculation	$R\log_2 R$
	Inverse covariance matrix	$N^2 + N\log_2 N$

Table 3 Computational complexity of the proposed and existing methods for various number of data sample points

No. of data points	Time in seconds	
	SPICE	SPICE_GS
64	21.33	0.75
128	29.62	0.86
256	51.23	0.92
512	72.97	1.61
1024	138.89	1.73
4096	265.61	1.91

4 Results

4.1 Simulation results

The examples are presented for simulated data to examine the computational complexity between direct and the proposed fast implementation of SPICE. The simulation parameters considered are as follows:

With N = 200 and C = 3, the data samples are generated, which contains the three exponentials at 0.3100 Hz, 0.3150 Hz and 0.1450 Hz, having amplitudes $q_1 = 10e^{j\varphi_1}$, $q_2 = 10e^{j\varphi_2}$, and $q_3 = 10e^{j\varphi_3}$ with a interval of 1 s. The phase values $\left\{\varphi_r\right\}_{r=1}^{3}$ are uniformly distributed in the range [0,

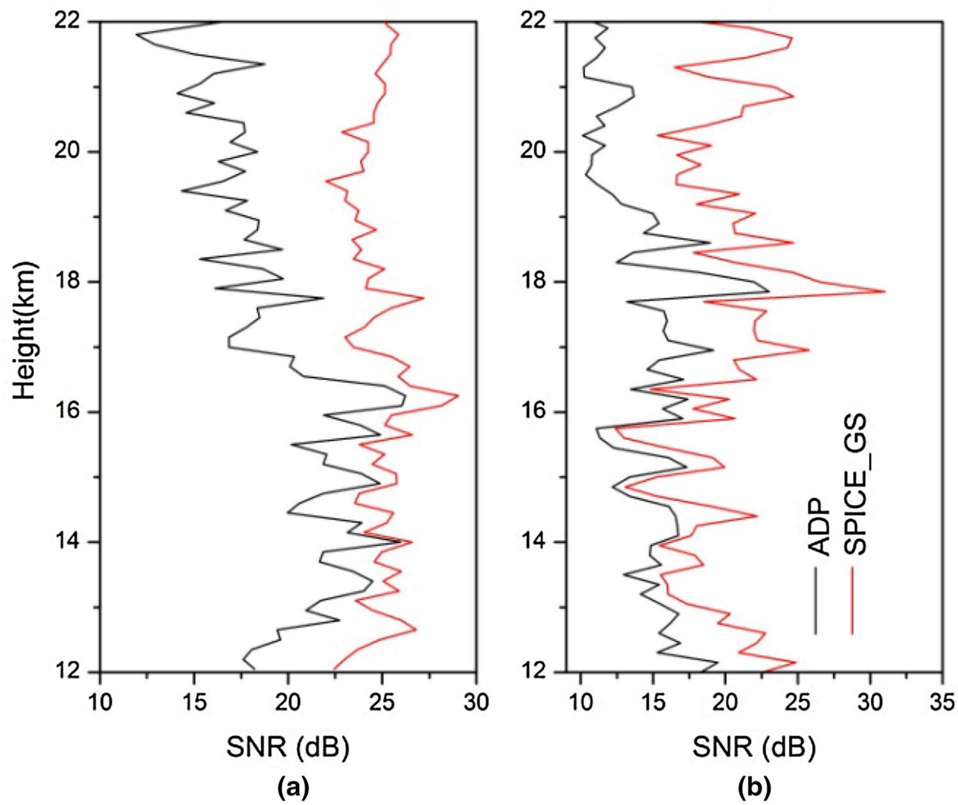

Fig. 2 Height profiles of SNR estimated using ADP and SPICE_GS for data obtained on Feb 9, 2015. **a** The east beam and **b** the south beam

2π]. The AWGN with zero mean and variance σ is added in the ε term.

The spectrum of the original signal before adding noise, computed using periodogram, implemented by SPICE and also implemented by fast SPICE_GS for SNR = -15 dB are shown in Fig. 1a–d respectively. It is apparent from the simulations, though the signal is entirely concealed in the noise, the SPICE methods, both direct implementation as well as Fast implementation, are able to estimate the parameters well. The periodogram is attained by padding 200 time series data points with 312 zeros and calculating the 512-point FFT. The number of points for processing for both techniques is 512.

The output SNR is estimated from the spectrum of the signal utilizing the noise level estimation method [16]. This is the widely used technique for noise threshold estimation and removal in atmospheric radar.

The simulations are carried on Intel Core i7-6700 CPU 3.4 GHz with 8 GB CPU memory. The comparison of the main operation process of SPICE and SPICE_GS are tabulated in Table 2. The computational complexity attained by the proposed method over the existing is illustrated in Table 3, for various data points.

4.2 Results for MST radar data

The radar data is gathered from the "Indian MST radar", which is operated at the NARL, Gadanki, Andhra Pradesh. This time-series data is subjected to the ADP, which normally uses the method of periodogram for the calculation of power spectrum. The output SNR estimated using ADP and SPICE_GS for east and south beams are depicted in Fig. 2.

Figure 3 shows the power spectrum at the range bins numbered 63 estimated using ADP and SPICE_GS for the east beam of Feb 9,2015 data. SPICE-GS identifies the particular frequency than the ADP which demonstrates the accuracy of the algorithm.

The zonal wind v_x, meridional wind v_y, and wind speed W components obtained using SPICE_GS, ADP and GPS radiosonde for the data on Feb 09, 2015, are depicted in the Fig. 4. From Fig. 4, it can be seen that the proposed SPICE_GS is following the GPS, especially in the range 14–17 km. However, the wind profile curves obtained using the ADP deviate from those obtained using GPS, in a considerable measure, after a height of 11 km. The direct implementation SPICE and the fast implementation SPICE_GS yields the same results and so we have shown the fast implementation results.

The comparison of the computational time of direct and fast implementation of SPICE for radar data processing is

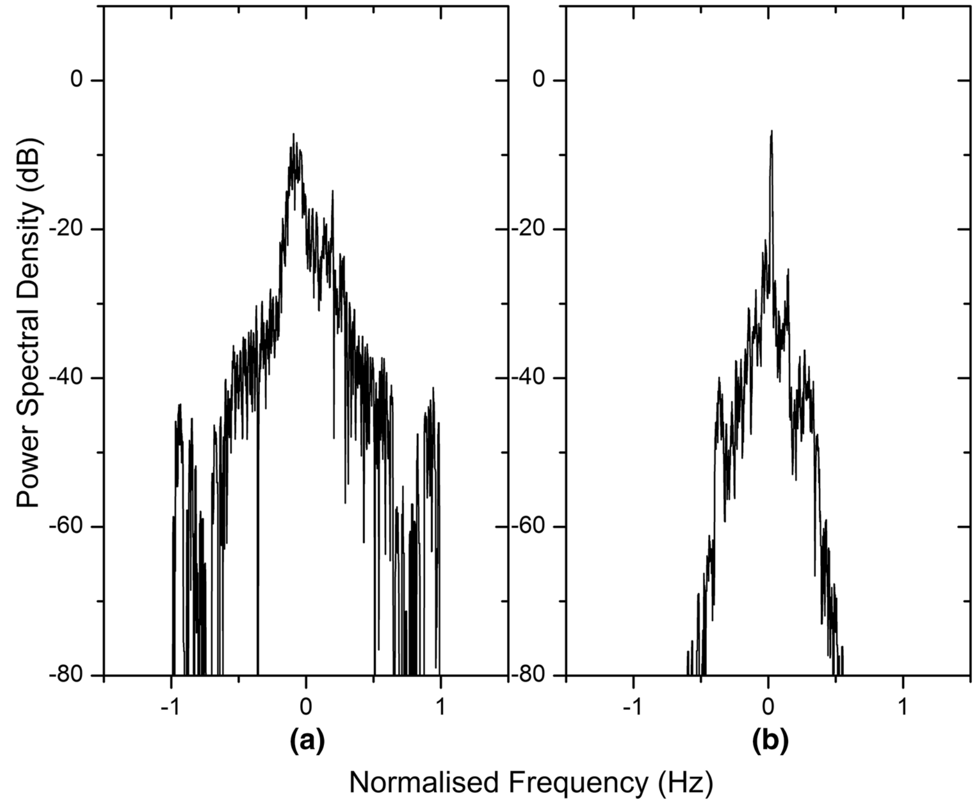

Fig. 3 Spectrum at bin 63 of the east beam for data obtained on Feb 9, 2015. **a** ADP and **b** SPICE_GS

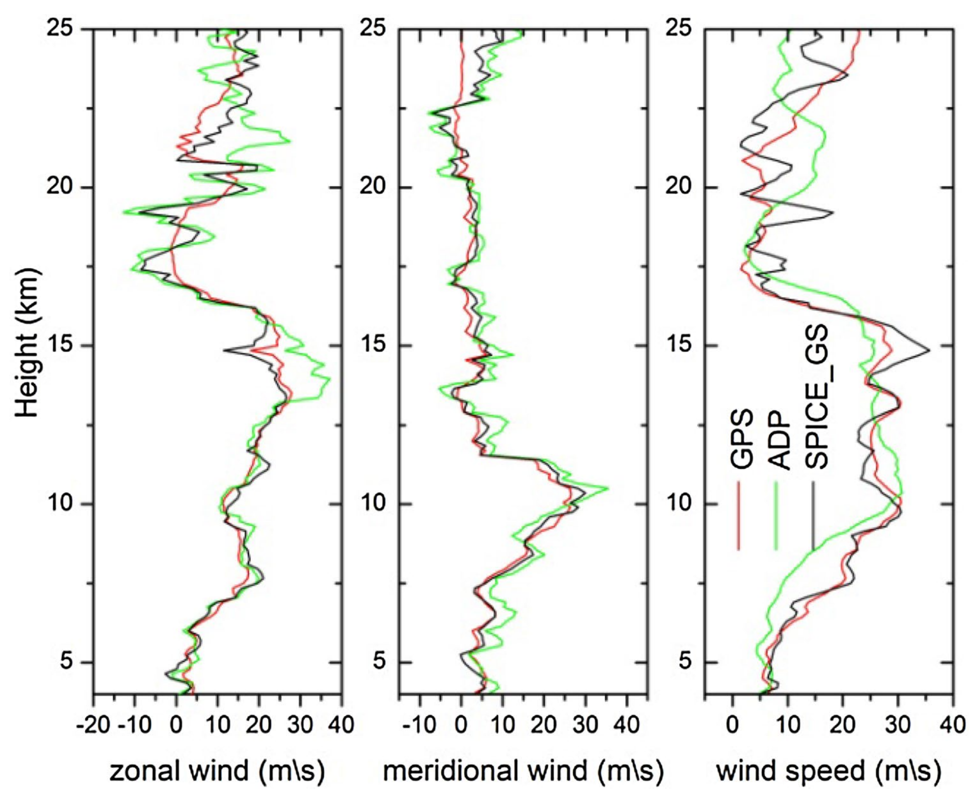

Fig. 4 Zonal, meridional and wind speed comparing GPS radiosonde, SPICE_GS and ADP

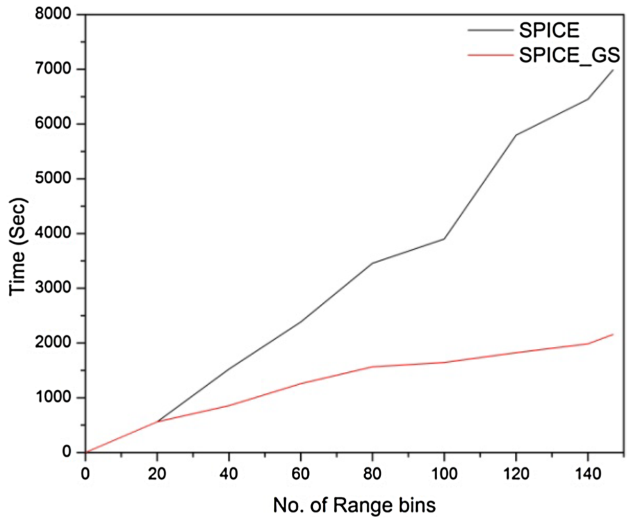

Fig. 5 Computational time comparison plot for processing MST radar data by SPICE and SPICE_GS

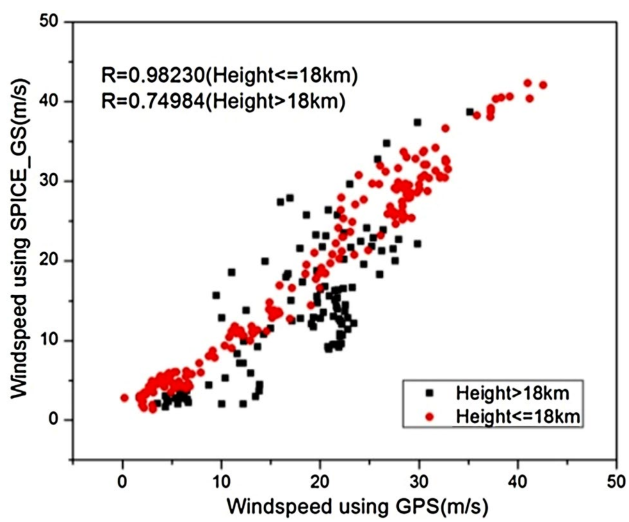

Fig. 6 Correlation between GPS wind speed and SPICE_GS wind speed

shown in Fig. 5 portraying a substantial time reduction in fast implementation than that of direct implementation, making the former striking.

Suitability of the method for processing the MST radar data is tested by correlation studies. The correlation between the GPS radiosonde data and SPICE_GS wind speed is displayed in Fig. 6 for the radar data retrieved during Feb 09–12, 2015. The correlation factor for height less than or equal to 18 km is 0.98230 and that for height greater than 18 km is 0.74984.

5 Conclusion

The fast implementation of semiparametric method for spectrum estimation, i.e., SPICE_GS, is applied to MST radar data retrieved from the NARL. Since the Gohberg–Semencul factorization of the covariance matrices is applied, we can leverage the Toeplitz/block-Toeplitz structure to compute the spectral estimate. The processed results have revealed noteworthy computational reductions. A considerable increase in computational efficiency has been obtained by SPICE_GS, devoid of the loss in performance.

Acknowledgements The authors thank National Atmospheric Research Laboratory (NARL), Gadanki for giving the radar data and CoE, ECE Department, SVUCE for technical assistance.

Compliance with ethical standards

Conflict of interest The author states that, there is no conflict of interest.

References

1. Stoica P, Moses RL (2005) Spectral analysis of signals. Prentice-Hall, Upper Saddle River, NJ
2. Stoica P, Babu P, Li J (2011) New method of sparse parameter estimation in separable models and its use for spectral analysis of irregularly sampled data. IEEE Trans Signal Process 59(1):35–47
3. Thatiparthi S, Gudheti R, Sourirajan V (2009) MST radar signal processing using wavelet-based denoising. IEEE Geosci Remote Sens Lett 6(4):752–756
4. Reddy T, Reddy GR (2010) MST radar signal processing using cepstral thresholding. IEEE Trans Geosci Remote Sens 48(6):2704–2710
5. Reddy TS, Reddy GR (2010) Spectral analysis of atmospheric radar signal using filter banks polyphase approach. Digit Signal Process 20(4):1061–1071
6. Rao DUM, Reddy TS, Reddy GR (2014) Atmospheric radar signal processing using principal component analysis. Digit Signal Process 32:79–84
7. Eappen NI, Sreenivasulu Reddy T, Ramachandra Reddy G (2016) Semiparametric algorithm for processing MST radar data. IEEE Trans Geosci Remote Sens 54(5):2713–2721
8. Raju C, Sreenivasulu Reddy T (2018) Sparse iterative covariance based estiamtion for atmospheric radar data. Int J Eng Technol (UAE) 7(1):232–236
9. Gohberg IC, Semencul AA (1972) On the inversion of finite Toeplitz matrices and their continuous analogs. Mat Issled 2:201–233 **(in Russian)**
10. Huckle T (1993) Computation of Gohberg–Semencul formula for a Toeplitz matrix. Technical report, University Wurzburg and Stanford University
11. Xue M, Xu L, Li J (2011) IAA spectral estimation: fast implementation using the Gohberg–Semencul factorization. IEEE Trans Signal Process 59(5):3251–3261
12. Hang Q, Abedia H, Xue M, Rowe W, Li J (2012) Fast Implementation of sparse iterative covariance-based estimation for source localization. J Acoust Soc Am 131(2):1249–1259

13. Jiang Xiaoyu, Hong Kicheon (2017) Gohberg–Semencul type formula and application for the inverse of a conjugate-Toeplitz matrix involving imaginary circulant matrices. J Nonlinear Sci Appl 10:2848–2859
14. Zheng Y, Shon S, Fu Z (2018) A Gohberg–Semencul type formula for the inverse of conjugate-Toeplitz matrix and applications. Acta Math Appl Sin Engl Ser 34:293–303
15. Jiang Z-L, Chen J-X (2017) The explicit inverse of nonsingular conjugate-Toeplitz and conjugate-Hankel matrices. J Appl Math Comput 53:1–16
16. Hildebrand PH, Sekhon R (1974) Objective determination of the noise level in Doppler spectra. J Appl Meteorol 13(7):808–811